Progress In Electromagnetics Research M, Vol. 119, 37–50, 2023

Star Shaped Fractal Conformal MIMO Antenna for WLAN, Vehicular and Satellite Applications

Chiranjeevi Reddy Sereddy[1, 3] and Usha D. Yalavarthi[2, *]

Abstract—A compact and novel star shaped fractal microstrip patch conformal MIMO antenna suitable for WLAN, vehicular communications (5.855–5.925 GHz), and Fixed Satellite Services (FSS) applications is proposed in this paper. The analysis of planar and conformal single element and four element MIMO antennas is presented. The proposed star shaped fractal MIMO antenna is prototyped on a polyamide substrate of geometry $104 \times 30 \times 0.4\,\text{mm}^3$. It achieves an impedance bandwidth ($S_{11} < -10\,\text{dB}$) of 3.7 GHz operating from 4.53–7.86 GHz. Radiation patterns and surface current distribution are investigated at 5.9 GHz and 7.3 GHz center frequencies. Peak gains of 5.42 dB and 4.86 dB are obtained at 5.9 GHz and 7.3 GHz, respectively. Radiation efficiency is more than 98%, and MIMO performance parameters are also analyzed. The proposed conformal MIMO antenna shows fine diversity performance for WLAN, vehicular and FSS communications.

1. INTRODUCTION

In recent years, much advancement has been done in vehicular communications. Most of vehicular communication uses Dedicated Short Range Communications (DSRC) frequency band in the range of 5.795–5.815 GHz for some applications and 5.855–5.925 GHz for a few other applications. The impact of 5G, fractal antennas on vehicular communications is presented in detail by the authors in [1]. Many researchers are working towards the design of flexible, fractal, and MIMO antennas for vehicular communications. Various antenna models proposed for vehicular applications are presented in [2–21]. A dual band antenna operating for WLAN and WAVE frequency bands is proposed in [2]. A wheel shaped transparent antenna with flexibility is presented for vehicular communications [3]. A multiband planar antenna with a wheel shaped structure is designed and analyzed in [4] for vehicular applications. A circularly polarized dual band antenna is presented in [5] for WLAN and vehicular applications. A metamaterial based conformal antenna with circular polarization is presented on a Liquid Crystal Polymer (LCP) substrate [6] for WiMAX, WLAN, and vehicular applications. A multiband coplanar waveguide fed transparent antenna is presented in [7] for automotive applications. A rectangular patch antenna with enhanced gain properties is presented [8] for automotive applications in C-band. A dual band flexible antenna for automotive communications and the effects of vehicular platform on it are presented and analyzed in [9]. A high gain Vivaldi antenna for 5G based Internet of vehicle communications is proposed and analyzed [10]. A flexible circularly polarized antenna is proposed for vehicle to everything communications in [11]. A printed monopole antenna with wideband characteristics is presented in [12] for 5G based vehicular wireless communications. A monopole antenna with tri-band characteristics is proposed in [13] for WiMax, WLAN, and WAVE applications. An ultra-wideband (UWB) monopole multiple-input multiple-output (MIMO) antenna with a defected ground structure (DGS) is designed for automotive applications [14]. A multiband array antenna for

Received 23 June 2023, Accepted 25 August 2023, Scheduled 14 September 2023

* Corresponding author: Usha Devi Yalavarthi (ushadevi.yalavarthi@kluniversity.in).

[1] Department of ECE, Koneru Lakshmaiah Education Foundation, AP, India. [2] Department of ECE, Koneru Lakshmaiah Education Foundation, AP, India. [3] Department of ECE, Rayalaseema University, Kurnool, AP, India.

DSRC applications is proposed in [15]. A defected ground structure based dual band array antenna is presented in [16] for intelligent transportation system (ITS) applications. A T-shaped MIMO antenna with complementary split ring resonators for 5G based vehicular communications is proposed in [17]. The authors in [18] present a slot-based MIMO antenna with broadband directional characteristics and analyze the performance of vehicular applications. A quad-element MIMO antenna with improved isolation and wideband performance is proposed in [19] for vehicular base station. A UWB transparent MIMO antenna is represented and analyzed for automotive communications in [20]. Flexible MIMO antennas with polarization diversity, multiband for sub-6 GHz and 5G, WLAN applications are presented in [21–24] for V2X communications. Various antenna models proposed and presented so far are very specific to vehicular communications. Microstrip patch antenna suitable for various applications like WLAN, V2X and FSS can be designed to further enhance the communication capability. MIMO antenna can overcome the spectral scarcity and can significantly improve data rates, link reliability, and overall communication performance. A conformal antenna integrated into the vehicle body will not disrupt the vehicle's aerodynamics or aesthetics. It also minimizes the impact on the vehicle's external appearance and functionality. Therefore, a conformal MIMO antenna operating for multiple applications like WLAN, V2X and FSS is desirable.

This paper proposes a star shaped fractal conformal MIMO antenna for WLAN (4.9, 5 and 5.9 GHz), vehicular communications (5.9 GHz), and Satellite applications (4–8 GHz C-band). Section 2 depicts the proposed single element antenna with fabrication model and results. Section 3 deals with the bending analysis of single element antenna and its performance. Section 4 describes 4-element collinear MIMO antenna simulation, prototype models, and results obtained. Section 5 gives the performance analysis of proposed conformal MIMO antenna wrapped onto cylindrical surface. Section 6 depicts the state-of-art literature comparison of presented conformal MIMO antenna with other recent appropriate works. Section 7 presents the conclusion of proposed work with significant results achieved.

2. STAR SHAPED FRACTAL ANTENNA

A microstrip patch antenna for vehicular communications is aimed to design in this section. The initial antenna design started with a basic star shaped microstrip patch antenna with full ground plane, and then four-star shaped elements are repeated as a fractal element to attain required operating characteristics. Star shaped fractal antenna iterations with truncated ground plane are presented in Figure 1. Iteration-1 is a star shaped antenna with full ground plane and truncated ground plane. The

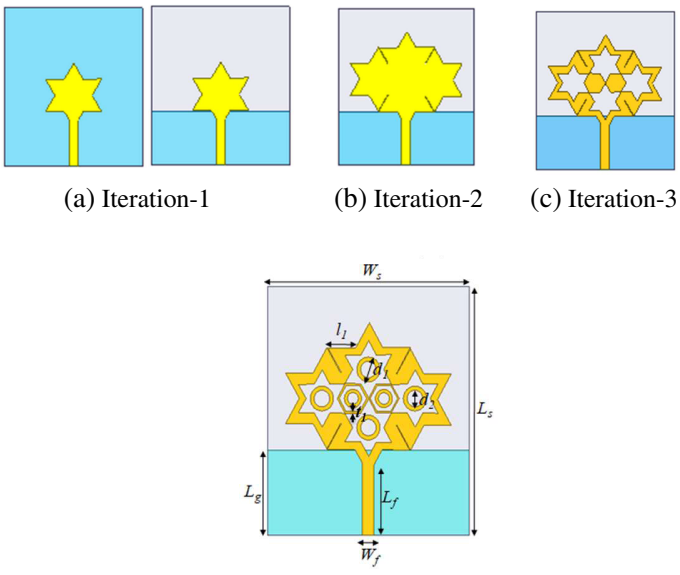

Figure 1. Star shaped antenna iterations.

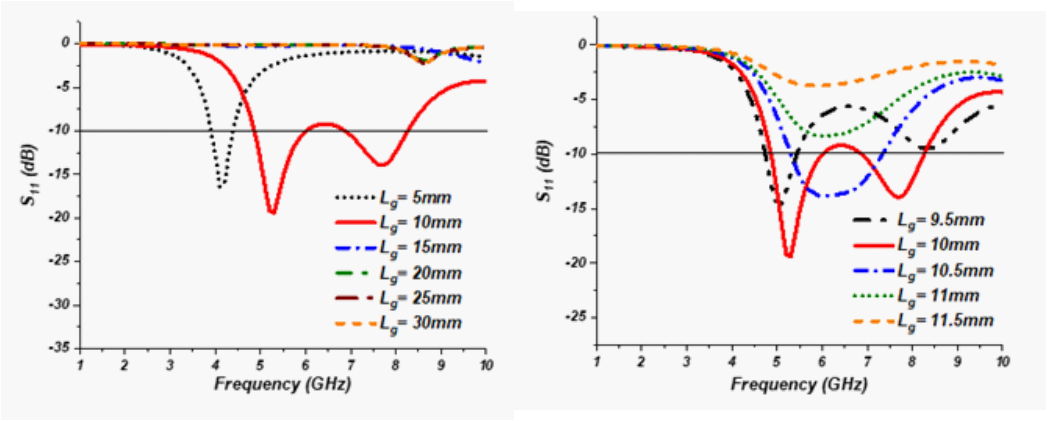

Figure 2. S_{11} characteristics of Iteration-1 for variations in length of ground plane L_g.

length of ground plane (L_g) affects the operating band of microstrip patch antenna. S_{11} characteristics of star shaped antenna iteration-1 for variations in the length of ground plane are illustrated in Figure 2.

For $L_g = 10$ mm, the proposed star shaped antenna achieved better operating band. Four-star shaped elements are repeated to attain a fractal structure in iteration-2. In iteration-3 stars are etched from each element, and in iteration-4 annular rings are placed in etched slots to enhance the operating characteristics and to achieve C-band (4–8 GHz) operating band that is suitable for WLAN, DSRC, and FSS applications. Proposed antenna iterations operating characteristics (S_{11}) are represented in Figure 3 for the initial feed width of 1.55 mm. For $S_{11} <= -10$ dB, iteration-1 operates for dual bands from 4.85–6.1 GHz and 6.85–8.27 GHz; iteration-2 operates from 3.86–4.89 GHz and 5.52–7.98 GHz; iteration-3 operates from 4.02–7.84 GHz; and iteration-4 operates from 3.95–8.09 GHz with an impedance bandwidth of 4.14 GHz. Proposed antenna feedwidth (W_f) is varied, and parametric analysis is done to obtain optimized antenna performance through S_{11} characteristics.

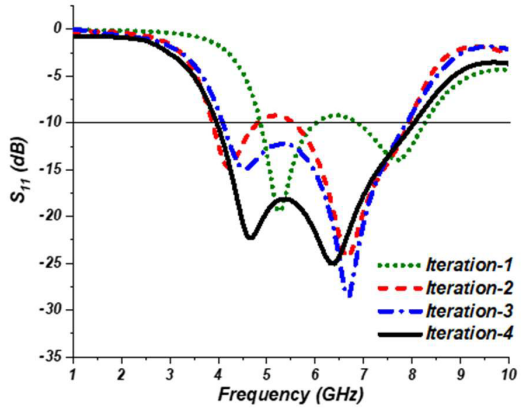

Figure 3. S_{11} characteristics of proposed star shaped antenna iterations.

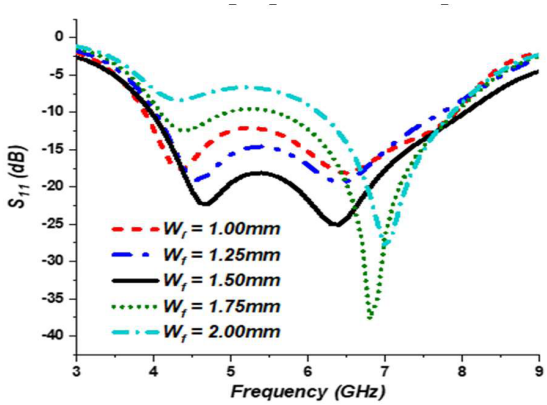

Figure 4. Parametric analysis of star shaped antenna for variations in W_f.

Figure 4 represents S_{11} characteristics of parametric analysis with respect to W_f. Feedwidth is varied in the range of 1–2 mm with step size of 0.25 mm. It is observed that optimum operating bandwidth is obtained for $W_f = 1.5$ mm. Geometrical specifications of proposed antenna in mm are depicted in Table 1. The proposed antenna is prototyped on a flexible polyamide substrate of dimensions 26 mm × 30 mm × 0.4 mm to achieve conformal properties suitable for vehicular communications. Fabricated antenna top and bottom views are illustrated in Figures 5(a) and 5(b). The prototype of proposed antenna is fabricated using photolithographic etching process. Fabricated antenna is tested

Table 1. Specifications of star shaped fractal antenna in mm.

Parameter	L_s	W_s	L_g	W_f	L_f	d_1	d_2	l_1	t_1
Dimensions (mm)	30	26	10	1.5	8.5	3	2	3.5	0.25

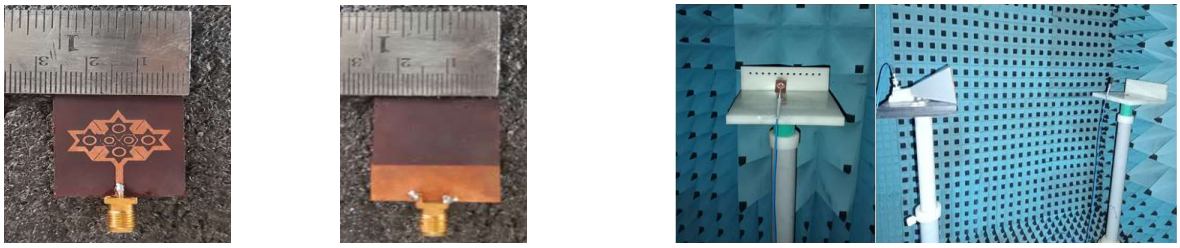

(a) Top view (b) Bottom view (c) Measurement in anechoic chamber

Figure 5. Fabricated star shaped fractal antenna.

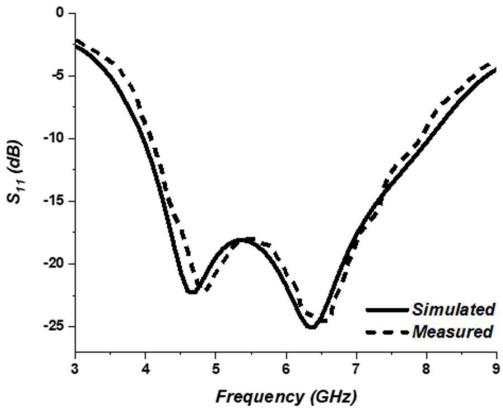

Figure 6. Simulated and measured S_{11} characteristics.

for validation using VNA and an anechoic chamber. Simulated and measured S_{11} characteristics are depicted in Figure 6, and the measured results are in good agreement with simulated ones.

Surface current distributions of the proposed star shaped antenna at 5.9 GHz and 7.3 GHz are represented in Figures 7(a) and (b), respectively. It is noticed that most current is distributed in feed line and star shaped fractal radiating element. Two-dimensional radiation patterns at 5.9 GHz are illustrated in Figure 8. Figure 8(a) gives radiation patterns in E-plane (co- and cross-polarizations). E-plane pattern is a dipole like pattern, and cross polarization is less than co-polarization. H-plane patterns are described in Figure 8(b). Co-polarization pattern is similar to omnidirectional patterns, and cross-polarizations is less than co-polarization. Figure 9 represents gain and radiation efficiency vs frequency features of star shaped fractal antenna. The antenna achieved 96% radiation efficiency and gain of 3.3 dB in operating band.

3. CONFORMAL STAR SHAPED FRACTAL ANTENNA

To validate the proposed antenna for conformal applications, bending analysis at different center bending angles 10°, 20°, 30°, 45°, 60°, and 90° is presented in this section for single element antenna. A collinear MIMO antenna is made conformal over a cylindrical surface, and performance parameters are analyzed. Figure 10 represents simulated bending models of proposed single element antenna at 45°, 90° and experimental setup for bending analysis.

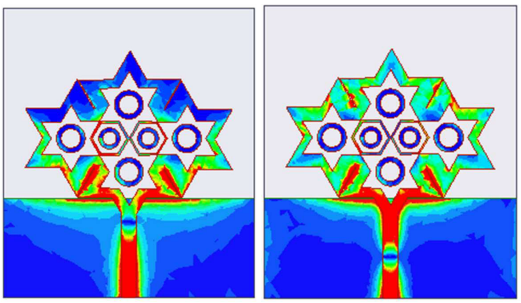

(a) 5.9 GHz (b) 7.3 GHz

Figure 7. Current distribution of star shaped fractal antenna.

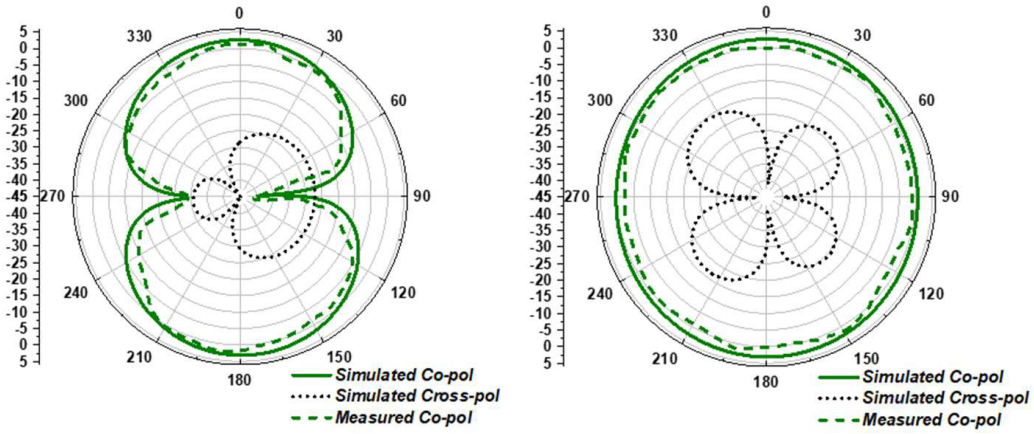

(a) E-plane radiation pattern (b) H-plane radiation pattern

Figure 8. Far field characteristics of star shaped fractal antenna at 5.9 GHz.

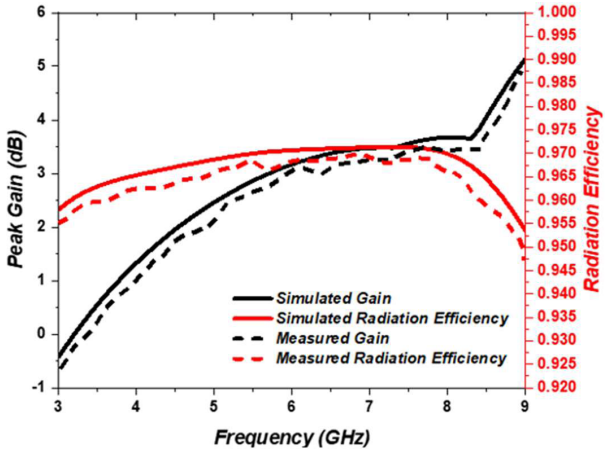

Figure 9. Gain and radiation efficiency of star shaped fractal antenna.

3.1. Analysis of Conformal Models

S_{11} characteristics of conformal single element antenna at different central bending angles are illustrated in Figure 11. It is observed that all conformal models work for 5.9 GHz DSRC vehicular communication

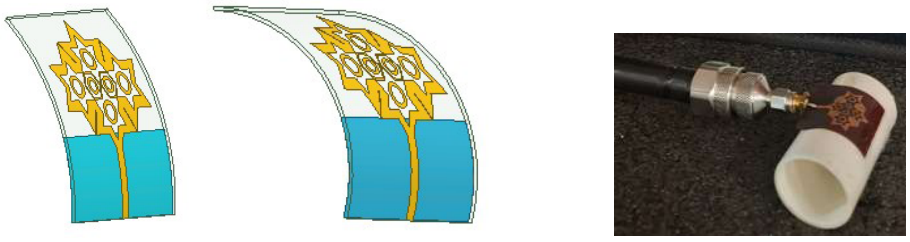

(a) 45° bending (b) 90° bending (c) Experimental set-up

Figure 10. Conformal models of star shaped fractal antenna.

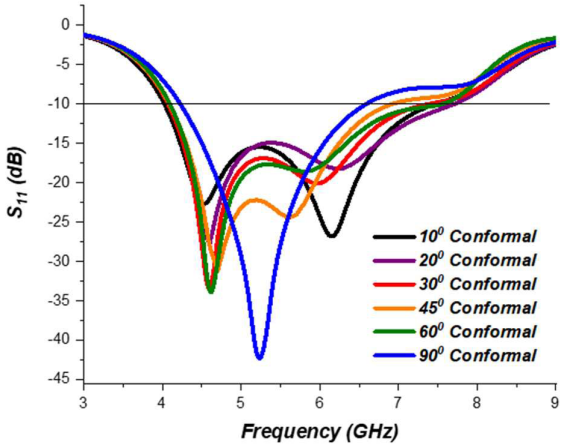

Figure 11. S_{11} characteristics of conformal models.

Table 2. Operating bands and bandwidth of conformal antenna models.

Bending Angle	Operating Band (GHz)	Bandwidth (GHz)	Gain (dB)	Radiation Efficiency (%)
Planar	4.10–8.00	3.90	3.12	97.06
10°	4.05–7.45	3.40	3.50	96.81
20°	4.07–7.71	3.64	3.54	96.03
30°	4.09–7.40	3.31	3.66	96.43
45°	4.09–6.95	2.86	3.63	96.32
60°	4.10–7.55	3.45	3.65	95.78
90°	4.25–6.55	2.3	3.56	95.96

frequency band, and hence the proposed antenna will be suitable to integrate onto vehicular body for communications. Respective operating bands, bandwidth, gain, and radiation efficiency at 5.9 GHz are tabulated in Table 2.

E-plane and H-plane radiation patterns of planar and conformal antenna models at bending angles 20°, 60° and 90° are presented in Figure 12. These patterns are investigated at 5.9 GHz resonant frequency. As the bending angle increases pattern tilting is observed in both E-plane and H-plane patterns. This is due to the bending of antenna and distribution of field components accordingly.

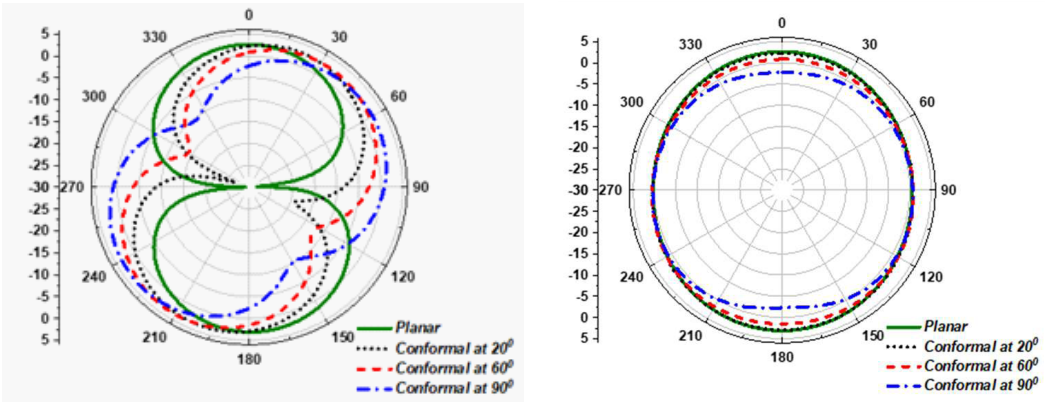

(a) E-plane (b) H-plane

Figure 12. Radiation patterns of conformal models at 5.9 GHz in E-plane and H-plane.

4. STAR SHAPED FRACTAL QUAD ELEMENT MIMO ANTENNA

MIMO antenna with four linear elements is proposed from a single element star shaped fractal antenna. The distance of separation between MIMO elements is $> \lambda/2$ to overcome coupling effects. To provide isolation, a 0.5 mm ground slot is etched between successive elements by keeping the connection between successive elements through 0.25 mm slot to avoid non-connected ground plane issues in MIMO antenna design. The simulated model of MIMO antenna and prototyped models are presented in Figure 13. MIMO antenna is fabricated on a polyamide substrate (104 mm $\times$ 30 mm $\times$ 0.4 mm).

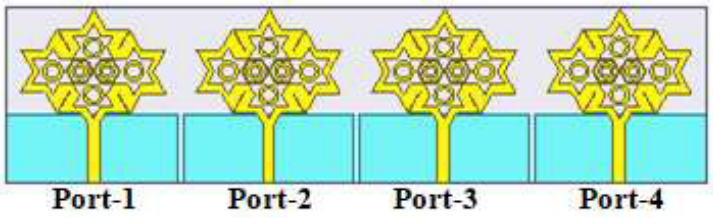

(a) Simulated model

(b) Fabricated model top view (c) Fabricated model bottom view

Figure 13. Four element collinear star shaped fractal MIMO antenna.

S-parameter characteristics of quad-element MIMO antenna are depicted in Figure 14 for port-1 excitation. Figure 14 illustrates simulated and measured S-parameters for port-1 excitation. An operating bandwidth (S_{11} <= -10 dB) of 3.7 GHz is obtained from 4.25–7.95 GHz. The minimum isolation between M_1 and M_2 is 20 dB, and the isolation between M_1 and M_3, M_1 and M_4 increases as the distance of separation increases in MIMO antenna arrangement. This behavior can be observed in Figure 14, S_{21}, S_{31} and S_{41} characteristics. S-parameter characteristics of proposed antenna for port-2

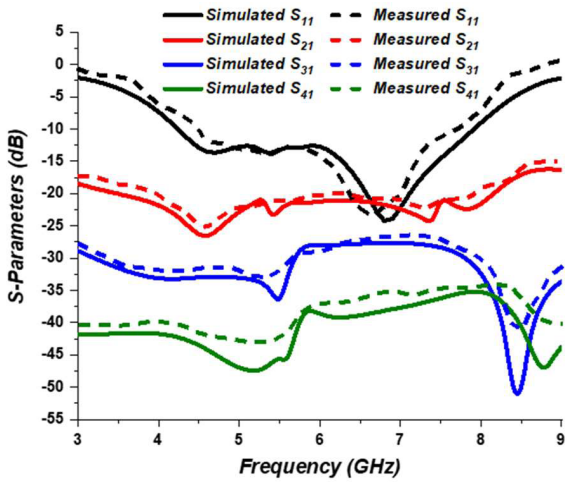

Figure 14. S-parameter characteristics of MIMO antenna.

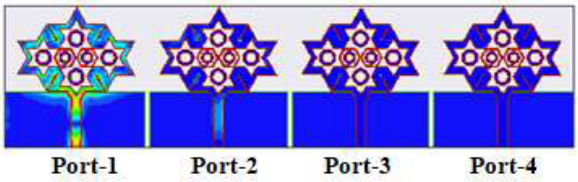

Figure 15. Surface current distribution at 5.9 GHz for port-1 excitation.

excitation are also investigated. It operates from 4.55–7.85 GHz, and the isolations between M_2 and M_1, M_2 and M_3 are close as both the elements are at same distance from M_2.

Figure 15 describes the surface current distribution for port-1 excitation at 5.9 GHz. When port-1 is excited, coupling with port-2 is minute whereas coupling with port-3 and port-4 is very low. Similarly, when port-2 is excited coupling with port-1 and port-3 is minute, and coupling with port-4 is very low. Therefore, the proposed antenna exhibits required isolation between MIMO elements.

5. CYLINDRICAL STAR SHAPED FRACTAL QUAD ELEMENT MIMO ANTENNA

Figure 16 presents cylindrical MIMO antenna with central bending angle of 360°. Figure 14(a) is the simulated model in HFSS, and Figure 16(b) is experimental setup of fabricated antenna. Figure 17 illustrates S-parameter features of proposed conformal cylindrical MIMO antenna for port-1 excitation.

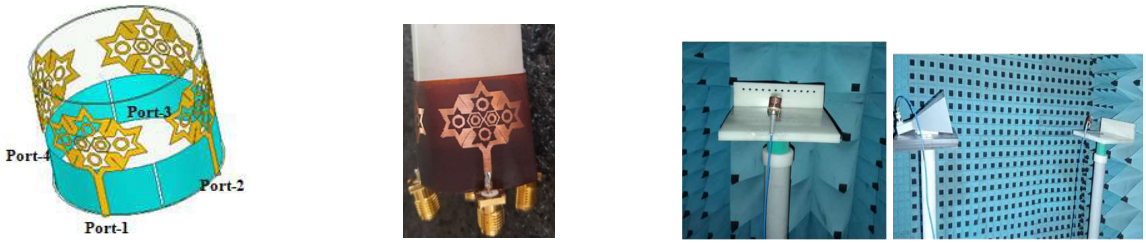

(a) Cylindrical MIMO antenna (b) Experimental set-up (c) Measurement in anechoic chamber

Figure 16. Conformal cylindrical star shaped fractal MIMO antenna.

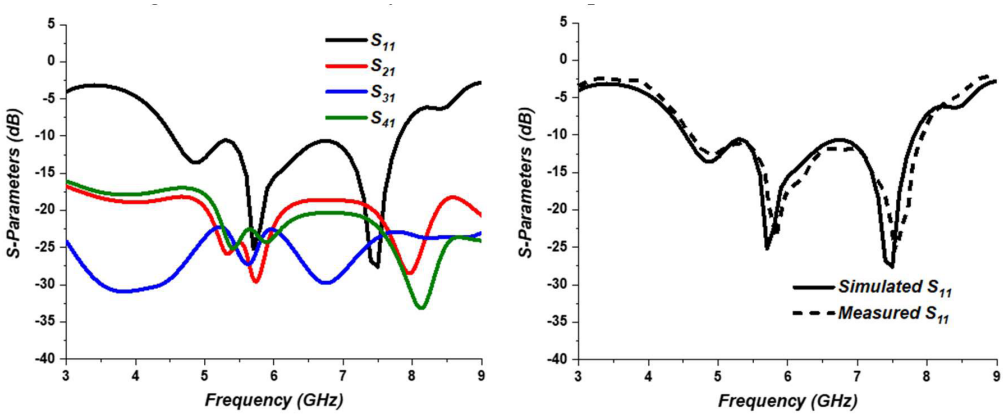

(a) Port-1 excitation (b) S_{11} characteristics

Figure 17. *S*-parameter curves of conformal cylindrical MIMO antenna.

It achieved operating band from 4.53–7.86 GHz with an impedance bandwidth of 3.33 GHz. Minimum isolation of 17.5 dB is achieved by the proposed antenna. Simulated and measured S_{11} features are in fine agreement as depicted in Figure 17(b).

Radiation patterns of conformal MIMO antenna at 5.9 GHz and 7.3 GHz frequencies in *E*- and *H*-planes are presented in Figure 18. Radiation patterns are directive in nature, and cross polarization is less than co-polarization. Far-field radiation characteristics of proposed conformal MIMO antenna are represented in Figure 19. A peak gain of 5.44 dB is attained at 5.8 GHz, and radiation efficiency is greater than 97.6% in operating band. Table 3 describes the antenna parameters of proposed star shaped quad-element conformal MIMO antenna in comparison with planar MIMO antenna.

Table 3. Planar MIMO and conformal cylindrical MIMO antenna parameters.

Parameter	Planar Collinear MIMO	Conformal cylindrical MIMO
Operating Band (GHz)	4.25–7.95	4.53–7.86
Bandwidth (GHz)	3.7	3.33
Gain (dB) at 5.9 GHz	3.98	5.42
Gain (dB) at 7.3 GHz	4.38	4.86
Radiation Efficiency (%) at 5.9 GHz	98.17	98.01
Radiation Efficiency (%) at 7.3 GHz	98.77	99.09
Isolation (dB)	> 20.5	> 17

5.1. MIMO Metrics

MIMO metrics envelope correlation coefficient (ECC) and diversity gain (DG) are presented in Figures 20 and 21 for port-1 excitation, respectively. These metrics give the analysis of diversity performance of proposed MIMO antenna. ECC can be calculated using Equation (1) in spherical coordinates $\Omega = (\theta, \varphi)$, and DG can be calculated from Equation (2) [24].

$$ECC = \frac{\left| \int_0^{2\pi} \int_0^{\pi} \left(XPRE_{\theta 1} E_{\theta 2}^* P_\theta + E_{\varphi 1} E_{\varphi 2}^* P_\varphi \right) d\Omega \right|^2}{\int_0^{2\pi} \int_0^{\pi} \left(XPRE_{\theta 1} E_{\theta 1}^* P_\theta + E_{\varphi 1} E_{\varphi 1}^* P_\varphi \right) d\Omega X \int_0^{2\pi} \int_0^{\pi} \left(XPRE_{\theta 2} E_{\theta 2}^* P_\theta + E_{\varphi 2} E_{\varphi 2}^* P_\varphi \right) d\Omega} \quad (1)$$

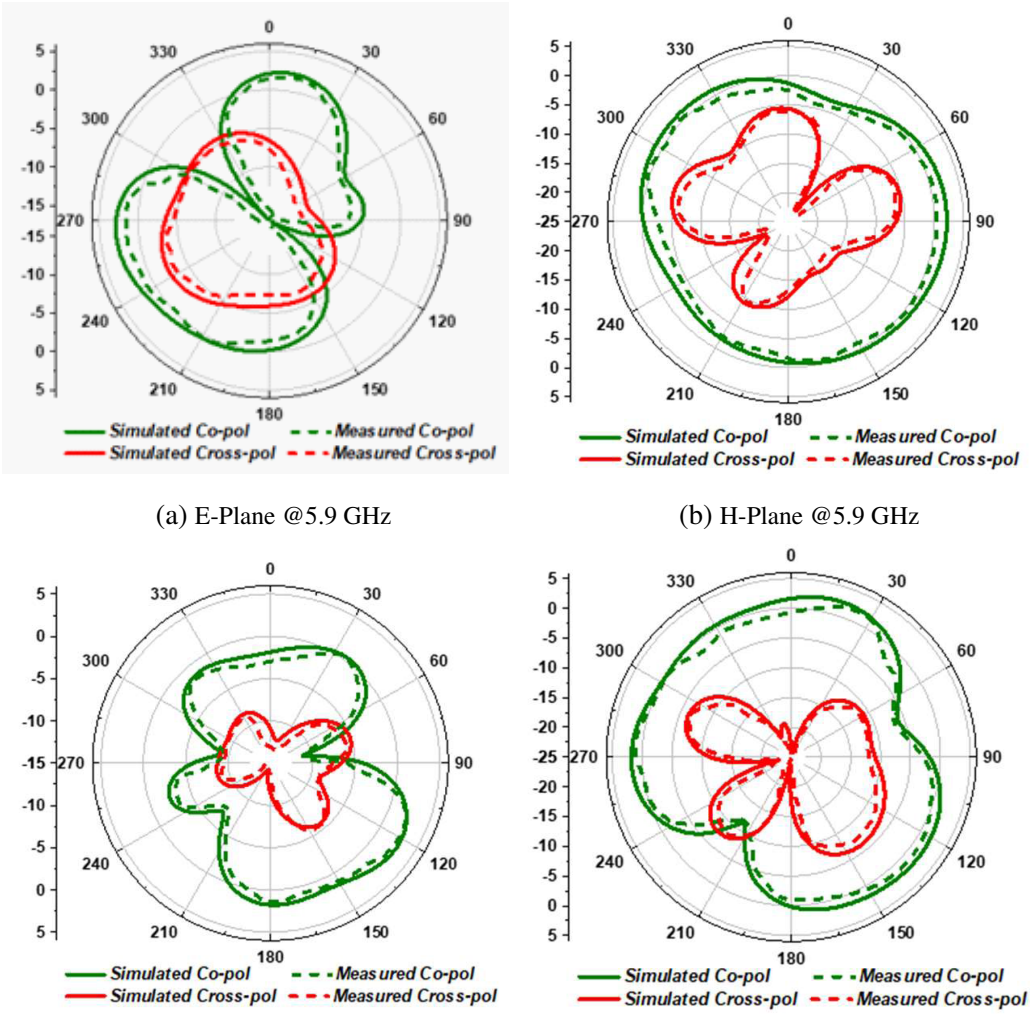

(a) E-Plane @5.9 GHz

(b) H-Plane @5.9 GHz

(c) E-Plane @7.3 GHz

(d) H-Plane @7.3 GHz

Figure 18. Radiation patterns of conformal cylindrical MIMO antenna.

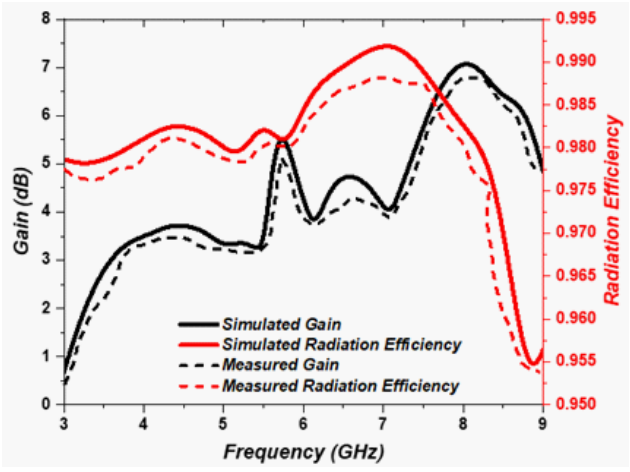

Figure 19. Gain and radiation efficiency of quad element conformal MIMO antenna.

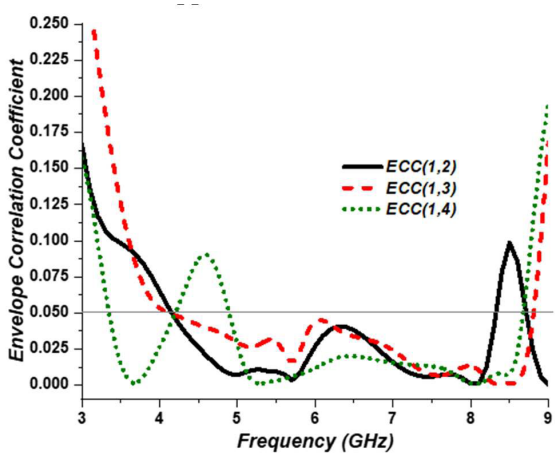

Figure 20. Envelope correlation coefficient.

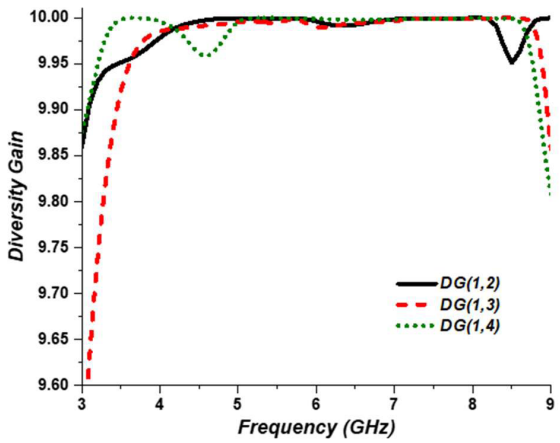

Figure 21. Diversity gain.

where $E_{\theta 1}$, $E_{\theta 2}$ are θ (vertical) polarized complex radiation patterns of antenna-1 and antenna-2 of the system, and $E_{\varphi 1}$, $E_{\varphi 2}$ are φ (horizontal) polarized complex radiation patterns of antenna-1 and antenna-2 of the system. XPR is cross-polar discrimination, defined as time-averaged vertical-to-horizontal power ratio.

$$DG = 10\sqrt{1 - ECC^2} \tag{2}$$

$ECC_{i,j}$ and $DG_{i,j}$ describe the diversity between port-i and port-j, where $i \neq j$. Due to symmetrical structures and uniform separation, $ECC_{i,j} = ECC_{j,i}$ and $DG_{i,j} = DG_{j,i}$. ECC and DG values for resonant frequencies 5.8 GHz, 5.9 GHz, and 7.3 GHz are given in Tables 4 and 5, respectively. $ECC < 0.05$ in operating band and DG is very close to 10. Therefore, the presented conformal cylindrical MIMO antenna exhibits good diversity performance characteristics suitable for WLAN, DSRC, and FSS applications.

Table 4. ECC values at different resonant frequencies.

Frequency (GHz)	$ECC_{1,2}$	$ECC_{1,3}$	$ECC_{1,4}$	$ECC_{2,3}$	$ECC_{2,4}$	$ECC_{3,4}$
5.8	0.008	0.021	0.007	0.0009	0.024	0.007
5.9	0.017	0.037	0.009	0.004	0.030	0.009
7.3	0.006	0.012	0.013	0.004	0.021	0.017

Table 5. DG values at different resonant frequencies.

Frequency (GHz)	$DG_{1,2}$	$DG_{1,3}$	$DG_{1,4}$	$DG_{2,3}$	$DG_{2,4}$	$DG_{3,4}$
5.8	9.99967	9.99767	9.99972	9.99999	9.99707	9.99969
5.9	9.99842	9.99292	9.99957	9.99990	9.99545	9.99958
7.3	9.99976	9.99925	9.99903	9.99990	9.99778	9.99847

6. STATE-OF-ART COMPARISON

Table 6 gives the comparison between state-of-art literature and proposed work in this paper. Proposed MIMO antenna is of its kind with conformability and MIMO metrics appropriate for DSRC vehicular communications, WLAN, and FSS applications.

Table 6. Comparison of presented work with appropriate works for vehicular communications.

References	Antenna Dimensions (mm^3)	Operating Band (GHz)	Substrate	Conformal	MIMO	Peak Gain (dB)
[3]	$40 \times 55 \times 3$	1.8–5.0, 5.5–6.4	Transparent PVC	✓	x	5.9
[5]	$40 \times 45 \times 1.6$	2.15–2.64, 5.27–6.18	FR-4	x	x	NA
[6]	$27.5 \times 23.2 \times 0.1$	3.4–3.78, 5.7–6.9	LCP	✓	x	NA
[13]	$24 \times 28 \times 1$	2.34–2.55, 3.39–3.69, 5.5–6.0	FR-4	x	x	3.7
[14]	$24 \times 16 \times 0.8$	3.1–10.9	FR-4	x	✓	3.5
[18]	$20 \times 10 \times 1.6$	3–6.75	FR-4	x	✓	4.97
[20]	$29 \times 24 \times 2.2$	2.4–11	Glass	x	✓	2
[22]	$20 \times 30 \times 0.635$	2.21–6	Melinex	✓	✓	0.53 dBi
[24]	$60 \times 60 \times 0.25$	2.6, 3.9, 5.6	Kapton Polyamide	✓	✓	4.1
Proposed Work	$26 \times 30 \times 0.4$	4.53–7.86	Polyamide	✓	✓	5.42

7. CONCLUSION

A flexible star shaped fractal MIMO antenna designed for vehicular applications is presented. The performance of single element antenna, its conformal models at different bending angles, four element collinear MIMO antenna, and its conformal cylindrical model are analyzed and presented. Cylindrical flexible MIMO antenna operates from 4.53–7.86 GHz suitable for WLAN, DSRC, and satellite applications. The presented MIMO antenna achieved fine diversity performance with isolation > 17 dB, ECC < 0.05, and DG close to 10. The gain at 5.9 GHz is 5.42 dB, and radiation efficiency is $> 98\%$. Therefore, the proposed conformal star shaped fractal antenna is well suitable for integrating onto vehicular body to support V2X communications. Further, the proposed conformal MIMO antenna can be integrated into vehicular surface and tested for vehicular communications.

REFERENCES

1. Rahim, A., P. K. Malik, and V. A. Sankar Ponnapalli, "State of the art: A review on vehicular communications, impact of 5G, fractal antennas for future communication," *Proceedings of First International Conference on Computing, Communications, and Cyber-Security (IC4S 2019). Lecture Notes in Networks and Systems*, P. Singh, W. Pawłowski, S. Tanwar, N. Kumar, J. Rodrigues, M. Obaidat, eds., Vol. 121, Springer, Singapore, 2020.

2. Liu, W.-C., C.-M. Wu, and N.-C. Chu, "A compact low-profile dual-band antenna for WLAN and WAVE applications," *AEU — International Journal of Electronics and Communications*, Vol. 66, No. 6, 467–71, Elsevier BV, Jun. 2012.
3. Madhav, B. T. P., T. Anilkumar, and S. K. Kotamraju, "Transparent and conformal wheel-shaped fractal antenna for vehicular communication applications," *AEU — International Journal of Electronics and Communications*, Vol. 91, 1–10, Elsevier BV, Jul. 2018.
4. Madhav, B. T. P. and T. Anilkumar, "Design and study of multiband planar wheel-like fractal antenna for vehicular communication applications," *Microwave and Optical Technology Letters*, Vol. 60, No. 8, 1985–93, Wiley, Jun. 2018.
5. Joshi, M. P. and V. J. Gond, "Design and analysis of microstrip patch antenna for WLAN and vehicular communication," *Progress In Electromagnetics Research C*, Vol. 97, 163–176, 2019.
6. Rao, M. V., B. T. P. Madhav, A. Tirunagari, and B. P. Nadh, "Circularly polarized flexible antenna on liquid crystal polymer substrate material with metamaterial loading," *Microwave and Optical Technology Letters*, Vol. 62, No. 2, 866–74, Wiley, Oct. 2019.
7. Trujillo-Flores, J. I., R. Torrealba-Meléndez, J. M. Muñoz-Pacheco, M. A. Vásquez-Agustin, E. I. Tamariz-Flores, E. Colin-Beltrán, and M. López-López, "CPW-fed transparent antenna for vehicle communications," *Applied Sciences*, Vol. 10, No. 17, 6001, MDPI AG, Aug. 2020.
8. Maddio, S., G. Pelosi, M. Righini, and S. Selleri, "A slotted patch antenna with enhanced gain pattern for automotive applications," *Progress In Electromagnetics Research Letters*, Vol. 95, 135–141, 2021.
9. Chletsou, A., J. F. Locke, and J. Papapolymerou, "Vehicle platform effects on performance of flexible, lightweight, and dual-band antenna for vehicular communications," *IEEE Journal of Microwaves*, Vol. 2, No. 1, 123–33, Institute of Electrical and Electronics Engineers (IEEE), Jan. 2022.
10. Kapoor, A., P. Kumar, and R. Mishra, "High gain modified vivaldi vehicular antenna for IoV communications in 5G network," *Heliyon*, Vol. 8, No. 5, e09336, Elsevier BV, May 2022.
11. Virothu, S. and M. S. Anuradha, "Flexible CP diversity antenna for 5G cellular vehicle-to-everything applications," *AEU — International Journal of Electronics and Communications*, Vol. 152, 154248, Elsevier BV, Jul. 2022.
12. Yacoub, A. M., M. O. Khalifa, and D. N. Aloi, "Wide band raised printed monopole for automotive 5G wireless communications," *IEEE Open Journal of Antennas and Propagation*, Vol. 3, 502–10, Institute of Electrical and Electronics Engineers (IEEE), 2022.
13. Dong, S. W., "A triple band C-shape monopole antenna for vehicle communication application," *Progress In Electromagnetics Research C*, Vol. 121, 97–106, 2022.
14. Alsath, M. G. N. and M. Kanagasabai, "Compact UWB monopole antenna for automotive communications," *IEEE Transactions on Antennas and Propagation*, Vol. 63, No. 9, 4204–08, Institute of Electrical and Electronics Engineers (IEEE), Sept. 2015.
15. Varum, T., J. Matos, P. Pinho, R. Abreu, A. Oliveira, and J. Lopes, "Microstrip antenna array for multiband dedicated short range communication systems," *Microwave and Optical Technology Letters*, Vol. 53, No. 12, 2794–96, Wiley, Sept. 2011.
16. Kishore, N., G. Upadhyay, V. S. Tripathi, and A. Prakash, "Dual band rectangular patch antenna array with defected ground structure for ITS application," *AEU — International Journal of Electronics and Communications*, Vol. 96, 228–37, Elsevier BV, Nov. 2018.
17. Venkateswara Rao, M., B. T. P. Madhav, et al., "CSRR-loaded T-shaped MIMO Antenna for 5G Cellular Networks and Vehicular Communications," *International Journal of RF and Microwave Computer-Aided Engineering*, Vol. 29, No. 8, Wiley, Apr. 2019.
18. Bactavatchalame, P. and K. Rajakani, "Compact broadband slot-based MIMO antenna array for vehicular environment," *Microwave and Optical Technology Letters*, Vol. 62, No. 5, 2024–32, Wiley, May 2020.
19. Wang, W., Z. Zhao, Q. Sun, X. Liao, Z. Fang, et al., "Compact quad-element vertically-polarized high-isolation wideband MIMO antenna for vehicular base station," *IEEE Transactions on Vehicular Technology*, Vol. 69, No. 9, 10000–08, Institute of Electrical and Electronics Engineers

(IEEE), Sept. 2020.

20. Potti, D., Y. Tusharika, M. G. N. Alsath, S. Kirubaveni, et al., "A novel optically transparent uwb antenna for automotive MIMO communications," *IEEE Transactions on Antennas and Propagation*, Vol. 69, No. 7, 3821–28, Institute of Electrical and Electronics Engineers (IEEE), Jul. 2021.
21. Virothu, S. and M. S. Anuradha, "Conformal MIMO circular polarization diversity antenna for V2X applications," *International Journal of RF and Microwave Computer-Aided Engineering*, Vol. 32, No. 4, Wiley, Dec. 2021.
22. Desai, A., M. Palandoken, J. Kulkarni, G. Byun, and T. K. Nguyen, "Wideband flexible/transparent connected-ground MIMO antennas for sub-6 GHz 5G and WLAN applications," *IEEE Access*, Vol. 9, 147003–147015, 2021, doi: 10.1109/ACCESS.2021.3123366.
23. Kulkarni, N. P., N. B. Bahadure, P. D. Patil, and J. S. Kulkarni, "Flexible interconnected 4-port MIMO antenna for sub-6 GHz 5G and X band applications," *AEU — International Journal of Electronics and Communications*, Vol. 152, 154243, 2022.
24. Saritha, V. and C. Chandrasekhar, "A conformal multi-band MIMO antenna for vehicular communications," *Progress In Electromagnetics Research Letters*, Vol. 108, 49–57, 2023.